

NATIONAL TRANSPORTATION SAFETY BOARD

Office of Research and Engineering
Materials Laboratory Division
Washington, D.C. 20594



April 22, 2013

MATERIALS LABORATORY FACTUAL REPORT

Report No. 13-026

A. ACCIDENT INFORMATION

Place : Pukoo, Hawaii
Date : November 10, 2011
Vehicle : Eurocopter EC130B4
NTSB No. : WPR12MA034
Investigator : Dennis Hogenson, AS-WPR

B. COMPONENTS EXAMINED

Fenestron attachment ring and a test block of material that was certified for use to manufacture a fenestron attachment ring.

C. DETAILS OF THE EXAMINATION

This report documents mechanical tests conducted on the fenestron attachment ring from the accident helicopter as well as mechanical tests conducted on a block of raw material supplied by Eurocopter. The test block of raw material had a conformance certificate showing that it met Eurocopter requirements for material used to manufacture a fenestron attachment ring. For more information regarding the Materials Laboratory examination of the fenestron attachment ring including fractography and metallography, see Materials Laboratory Factual Report 12-089.

The fenestron attachment ring fractured from the tail boom with a circumferential fracture located in the forward flange of the attachment ring. The location of the circumferential fracture of the forward flange is indicated in figure 1. The forward flange portion of the attachment ring remained attached to the tail boom and was exposed to heat from a post-crash fire. As shown in figure 1, the aft portion of the fenestron attachment ring with attached pieces of the fenestron skin was not exposed to heat or fire, and the aft flange of the fenestron attachment ring was intact at the right side of the fenestron.

According to the engineering drawing for the fenestron attachment ring, the attachment ring is machined from a plate of aluminum alloy 7010-T7451. In the manufacturing process, the rolling plane normal vector is oriented parallel to the longitudinal axis of the ring. The orientation of the rolling direction relative a clock position on the attachment ring is not specified. With the attachment ring in this orientation relative to the original plate, the circumferential plane of the attachment ring

is parallel to the short transverse plane for the plate,¹ and tensile loads for the short transverse loading condition are applied parallel to the longitudinal axis of the attachment ring.

Tensile Tests

The objective of the tensile tests was to obtain tensile properties of the accident attachment ring in the short transverse loading direction and relate those results to Eurocopter tensile property requirements for the specified fenestron attachment ring material. The tensile tests for certification and material conformance are determined using a standard round tensile specimen with an 8-mm-diameter reduced section and a 40-mm gage length tested in accordance with European Standard EN 2002-1:2005. However, a standard test specimen could not be machined from the manufactured component. Since test specimen geometry can have a significant effect on test results, a block of the material used to manufacture a fenestron ring was used to manufacture both standard round test specimens and custom-designed flat test specimens. The flat test specimens were specifically designed to fit within available material on the aft flange of the accident part. A dashed line in figure 1 bounds the area of the aft flange on the right side of the attachment ring from which the flat test specimens were cut.

All testing was conducted at Engineering Systems, Inc., (ESI) Norcross, Georgia. Tensile tests for both specimens were conducted in accordance with European Standard EN 2002-1:2005 where applicable and then in accordance with ASTM B557 or ASTM B557M where additional clarification to the European standard was needed. The standard test specimen had a round reduced section with an 8-mm diameter and a 40-mm gage length. A drawing of the custom test specimen is shown in figure 2. The custom test specimen had a rectangular reduced section with a width of 0.125 inch and a nominal thickness of 0.063 inch. The gage length of the custom test specimen was 0.5 inch, and the overall length was 1.5 inches.

Test Block Specimens

A view of the test block supplied by Eurocopter as cut from a plate of certified material is shown in figure 3. As received, the block was 3.8 inches (98 mm) thick. A piece of the block was cut from the corner, and three faces were polished and etched to determine the rolling direction, which is indicated in figure 3. As shown in figure 3, the rolling direction was approximately parallel to the longest edges of the block, and the short transverse loading direction was parallel to the shortest edges of the block.

Prism-shaped blanks were cut from the test block to prepare tensile specimens to compare tensile test results of the standard round specimens to those of the custom flat specimens for the same material. Final machining of the tensile specimens from the

¹ For the same cross-section, tensile specimens loaded in the short transverse direction (perpendicular to the rolling plane) are generally slightly weaker and show less ductility than specimens loaded in other directions oriented parallel to the rolling plane. Strength and ductility for the short transverse direction were included in the fenestron attachment ring design.

blanks was completed at ESI prior to testing. All specimens were oriented such that they were loaded in the short transverse loading direction. The standard round specimens had a total length equal to the thickness of the plate, and the custom flat specimens had dimensions shown in figure 2.

Five standard round specimens and 10 custom flat specimens were fabricated from the test block and then tested. Among the 10 custom flat specimens, 5 of the specimens were oriented such that the gage width was parallel to the rolling direction, and the other 5 specimens were oriented such that the gage width was perpendicular to the rolling direction. Table 1 lists results of the tensile tests conducted on the block of certified material. The ESI test report and tensile curves for the tests are included in Appendix A of this report.

Table 1. Test Block Tensile Test Results

Specimen Label*	Yield Strength (ksi)	Tensile Strength (ksi)	Total Elongation in 40 mm (Round) or 0.5 inch (Flat) (%)
Standard			
RND 1	68.0	75.0	7.9
RND 2	68.0	74.5	8.3
RND 3	67.5	74.0	8.2
RND 4	67.5	74.5	7.9
RND 5	67.0	74.0	7.6
Average of 5	67.6	74.4	8.0
Custom			
F1L	65.0	76.0	8.0
F2L	66.5	77.5	7.4
F3L	64.5	76.0	8.0
F4L	66.0	76.5	8.2
F5L	66.0	76.5	7.6
F1T	66.0	77.5	7.0
F2T	67.0	77.0	8.1
F3T	66.5	78.0	7.4
F4T	65.5	76.0	8.6
F5T	67.5	77.5	8.5
Average of 10	66.0	76.9	7.9

*RND indicates standard round specimen. F indicates custom flat specimen. L indicates specimen with gauge width oriented parallel to the rolling direction. T indicates specimen with gauge width oriented perpendicular to the rolling direction.

The measured average yield strength of the standard round specimens was 67.6 ksi² and the average tensile strength was 74.4 ksi. The average total elongation in the 40-mm gauge length was 8.0%. Documentation for the plate indicated the plate thickness for certification was 102 mm. The Eurocopter tensile property requirements for 102-mm thick plate of 7010-T7451 in the short transverse loading condition include a minimum yield strength of 54.4 ksi (375 MPa), a minimum tensile strength of 64.5 ksi (445 MPa), and a minimum total elongation of 3%. The mechanical properties of the test block measured using the standard round test specimen satisfied the requirements for tensile properties in the short transverse loading condition.

Comparing test results for the custom test specimens to the standard test specimens, the custom flat specimens had an average yield strength that was slightly lower and a tensile strength that was slightly higher than the standard round specimens. Average total elongation of both specimen types was nearly equal. The mechanical properties of the test block measured using the custom flat test specimen satisfied the requirements for tensile properties in the short transverse loading condition.

Fenestron Attachment Ring Specimens

A piece of the fenestron attachment ring aft flange was cut from the right side of the attachment ring as indicated with dashed lines in figure 1. Then, rivets attaching the fenestron attachment ring to the fenestron skin piece were removed by drilling. The resulting piece of the fenestron attachment flange used to fabricate the custom tensile specimens is shown in figure 2. Next, nine tensile specimen blanks were cut from the flange. The specimen blanks had a width approximately equal to the width of the grip section of the tensile specimens. The blanks were cut from the middle and upper portion of the flange piece shown in figure 2.

As per the engineering drawing for the fenestron attachment ring, the aft flange of the attachment ring had a tapered thickness where the end closest to the rib at the middle of the ring was thicker than the aft end of the flange. In addition, as evident in figure 2, the flange piece was curved. The taper and curvature were present on the tensile specimen blanks cut from the flange. In order to properly test the specimens, the taper and curvature had to be removed. The specimen blanks were placed in a vice, and the curvature was removed by hand using a crescent wrench. Specimens 1 and 2 were largely free of curvature. Specimens 6 and 9 had the greatest amount of curvature among specimens fabricated for testing.

Next, the specimen blanks were placed on a flat surface in a vice, and the painted exterior sides of the blanks were milled parallel to the interior surfaces to remove the thickness taper. The milled surface was then finished by sanding by hand with 800-grit silicon carbide paper. The interior surface of each specimen was retained as-fabricated from the original manufacture of the attachment ring. Finally, the mill was used to cut the reduced sections of the custom tensile specimens to create 7 tensile specimens numbered 1 through 6 and 9. Specimens were not fabricated from blanks

² The unit of ksi equals 1,000 pounds per square inch.

labeled 7 and 8. Marks showing the 0.5-inch gauge section were punched into the surface using the mill.

The tensile specimens were placed in grips in a load frame, and an extensometer with a 0.5-inch gauge length was attached to the side of the specimen. Views of one of the test specimens loaded in the test frame are shown in figure 4. The tests were conducted at a constant cross-head speed set to produce an engineering strain rate of 0.5% per minute up to yield, and then the speed was adjusted to produce an engineering strain rate of up to 10% until fracture.

A total of 6 specimens were tested to failure from the 7 tensile specimens that were fabricated. The fracture in specimen 2 occurred through one of the marks for the gauge section, so data from that specimen was not included in the results. Specimen number 3 slipped from the grips at a load close to the yield strength, and testing of that specimen was discontinued at that point. Specimens 5 and 6 slipped from the grips at loads below the yield strength, and these specimens were reloaded and tested to failure. Specimen 5 slipped at 27.2 ksi was reloaded and slipped again at 35.3 ksi before testing to failure. Specimen 6 slipped at 27.8 ksi before it was reloaded and tested to failure.

Results from the tensile tests of the custom flat tensile specimens from the fenestron attachment ring are listed in Table 2. Appendix B of this report contains the ESI test report and tensile curves for the completed tests. It is noted that fracture occurred near a gauge mark in specimens 6 and 9. While the total elongation for samples 6 and 9 are reported in table 2, some of the plastic deformation may have occurred outside of the gauge section, thus explaining the lower total elongation values measured for these two samples.

Table 2. Fenestron Attachment Ring Tensile Test Results

Specimen Number	Yield Strength (ksi)	Tensile Strength (ksi)	Total Elongation in 0.5 inch(%)
1	59.5	71.5	7.4
4	57.5	67.5	8.8
5	62.0	71.0	9.0
6	59.0	66.0	3.2
9	59.5	72.0	6.4
Average	59.5	72.0	7.0

According to the source material records for the fenestron attachment ring, the plate used to fabricate the fenestron attachment ring was 100 mm thick. The specified tensile properties in the short transverse loading direction for a 100 mm thick plate of 7010-T7451 used for the fenestron are a minimum yield strength of 56.6 ksi (390 MPa), a minimum tensile strength of 66.7 ksi (460 MPa), and a total elongation greater than

3%. As shown in table 2, the tensile specimens tested from the fenestron attachment ring generally satisfied the requirements for tensile properties in the short transverse loading direction. However, specimen 6 had a tensile strength that was less than 1 ksi below the specified minimum tensile strength. However, factors including specimen geometry, sample size, straightening operations, etc. should be considered when making an assessment of conformance with the minimum standards based on these tests.

Fractography

A fractographic examination was completed on selected flat samples from the test block and fenestron fitting. The examination provided a reference for fracture features expected for this material from an overstress tensile load in the short transverse loading direction. In addition, fractographic features associated with crack-like grain boundary pits were explored on the tested samples from the fenestron attachment ring.

Test Block Specimens

Overall views of the standard round and the custom flat specimens after testing are shown in figure 5. The fracture features of all the specimens generally showed a mix of matte gray and somewhat reflective fracture features on slant planes. Specimens F1L and F1T were arbitrarily chosen for a closer examination of fracture features.

Optical views of the fracture surfaces on the shorter ends of fractured specimens F1L and F1T are shown in figure 6. The difference in orientation with respect to rolling direction was evident in the fracture features. Terrace-like features associated with grain orientation were generally aligned with the width direction in specimen F1L, and the features were more aligned with the through-thickness direction in specimen F1T.

The fracture surfaces were examined using a scanning electron microscope (SEM). Typical fracture features observed on the F1L and F1T specimens are shown in figures 7 and 8, respectively. Fracture features generally appeared like plateaus or terraces with relatively flat areas between step changes in the fracture plane. These features were consistent with fracture along the grain boundaries in the short transverse plane. The flat areas between the steps generally showed fine equiaxed dimples interspersed with areas of larger irregular-shaped dimples. The tear ridges around the dimples were uniform around the perimeter of the dimple. Lighter-gray second-phase particles³ were frequently noted at the middle of the larger dimples, and the shape of the dimple corresponded to the shape of the second-phase particle. In some areas, the larger dimples and second-phase particles were found in clusters such as shown in figure 8.

³ The particles represent a local area with a different chemistry denoted as a second phase. The particles appear lighter due to a higher concentration of elements with a higher atomic weight (copper) relative to the surrounding material (mostly aluminum).

Fenestron Attachment Ring Specimens

An overall view of specimens from the fenestron attachment fitting after testing is shown in figure 9. A label indicating the specimen number is shown below each specimen. Test specimen 3 is intact as shown in figure 9. Specimens 7 and 8 were not fabricated and tested, and therefore they are not shown in the image. The fracture features of all the specimens generally showed a mix of matte gray and somewhat reflective fracture features on slant planes.

Test specimens 1 and 4 were arbitrarily chosen for a closer examination of fracture features, and optical views of the fracture surface on the shorter end of fractured test specimens 1 and 4 are shown in figure 10. The orientation of the step features on the fracture surface was consistent with the orientation of the specimen relative to the rolling direction. In test specimen 1, the rolling direction is mostly aligned with the width of the fracture face, whereas the rolling direction for specimen 6 was oriented at an angle relative to the specimen face. The approximate rolling direction based on fracture features is indicated in figure 10. The difference in rolling direction is a consequence of the position from which the specimen was removed on the curved surface of the fenestron attachment ring aft flange.

The fracture surfaces were examined using a scanning electron microscope (SEM). Typical fracture features observed on test specimen 1 from the fenestron attachment ring are shown in figures 11 and 12. Fracture features were generally similar to those observed on the test block samples with a terraced appearance at lower magnification and a mix of dimple features observed at higher magnification.

Secondary cracks were observed on the as-manufactured surface adjacent to the fracture as indicated in the lower image in figure 12. On the fracture surface adjacent to the as-manufactured surface, areas appearing relatively dark when imaged using backscattered electrons in composition mode⁴ were observed across portions of the fracture surface edge as shown in figures 13 and 14. The darker areas were consistent with oxides associated with grain boundary etching pits. The crack-like pits and oxidation at the grain boundaries occurred during the manufacturing process where the machined part is chromic acid anodized after an etching step is used to prepare the surface.

Typical SEM images of fracture features observed on test specimen 4 from the fenestron attachment ring are shown in figures 15 and 16. Fracture features were generally similar to those observed on the test block samples with a terraced appearance at lower magnification and a mix of dimple features observed at higher magnification.

⁴ SEM images produced using a backscatter detector in composition mode have contrast that is associated with atomic weight of the elements in the image. Materials with elements having higher atomic weights appear relatively lighter than others having elements with lower atomic weights.

Secondary cracks were observed on the as-manufactured surface adjacent to the fracture as indicated in the lower image in figure 16. On the fracture surface adjacent to the as-manufactured surface, areas appearing relatively dark when imaged using backscattered electrons in composition mode⁵ were observed across portions of the fracture surface edge as shown in figure 17. The darker areas were consistent with oxidized grain boundaries associated with etching pits that formed during the manufacturing process.

Metallography

The smaller ends of fractured test specimens 1 and 4 from the fenestron attachment ring were mounted in a metallurgical mount and polished in a plane parallel to the edge face (thin side) of the tensile specimen. The polished cross-sections were then etched with Keller's reagent.⁶ Images of the polished and etched cross-sections are shown in figures 18 and 19. The upper images in figures 18 and 19 show features adjacent to the fracture surface for specimens 1 and 4, respectively. Crack-like grain boundary etch pits were observed at the as-manufactured surface. The etch pits showed oxidation on their surfaces consistent with the chromic anodized surface. The lower images in figures 18 and 19 show some of the deepest oxidized grain boundary etch pits observed in the polished and etched cross-sections. The deepest etch pit in specimen 1 shown in figure 18 was 0.0019 inch deep, and the deepest etch pit in specimen 4 shown in figure 19 was 0.0016 inch deep.

Matthew R. Fox
Senior Materials Engineer

⁵ SEM images produced using a backscatter detector in composition mode have contrast that is associated with atomic weight of the elements in the image. Materials with elements having higher atomic weights appear relatively lighter than others having elements with lower atomic weights.

⁶ Keller's reagent is a mixture of nitric acid, hydrochloric acid, and hydrofluoric acid used to reveal grain boundaries in aluminum alloys.



Figure 1. Overall view of the fenestron attachment ring with attached pieces of fenestron. A dashed line indicates the area of the aft flange of the attachment ring where tensile test specimens were fabricated.

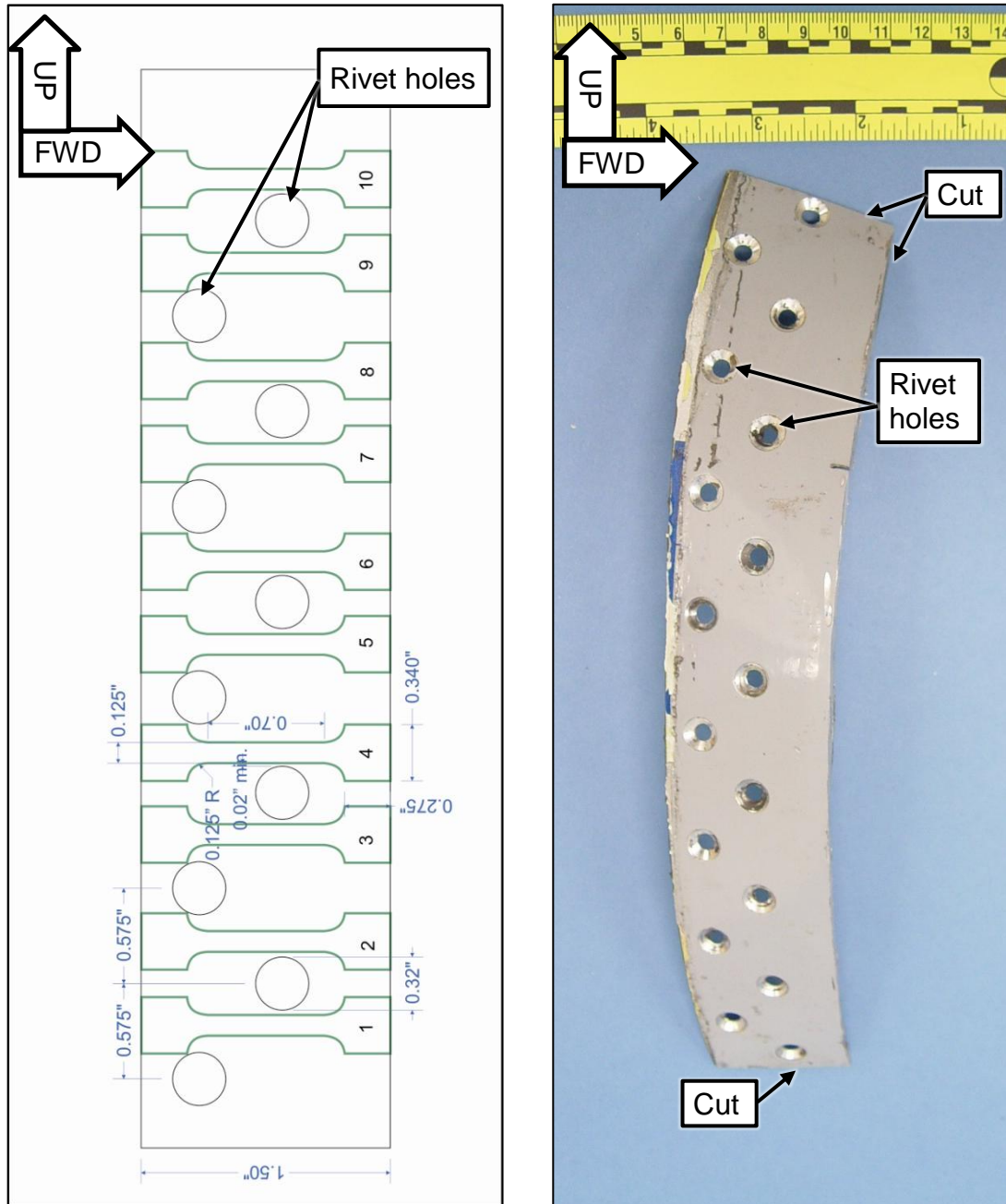


Figure 2. Drawing of the custom tensile specimens with dimensions showing locations on the aft flange of the attachment ring where 10 specimens could be removed (left) and piece of aft flange with rivets removed and cut as shown to facilitate machining of tensile specimens.

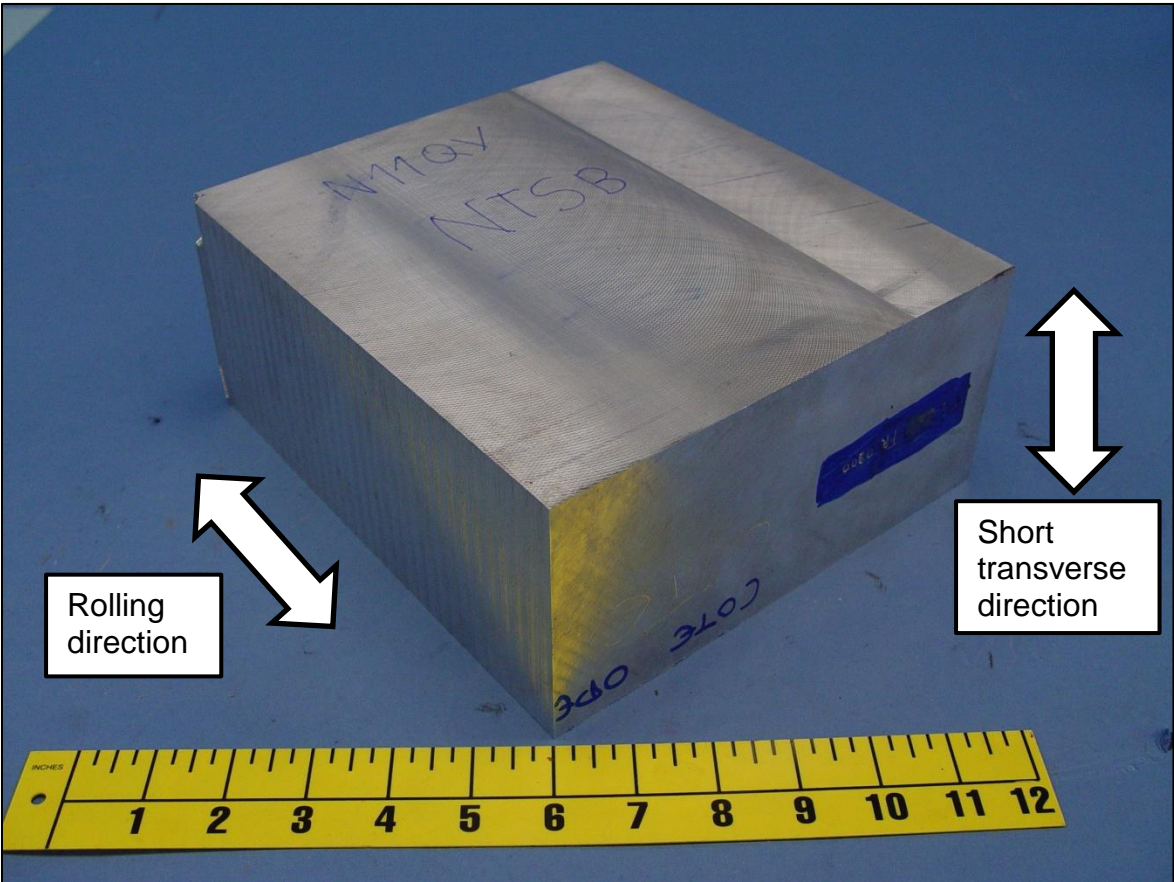


Figure 3. Overall view of the block of certified material supplied by Eurocopter for tensile tests.

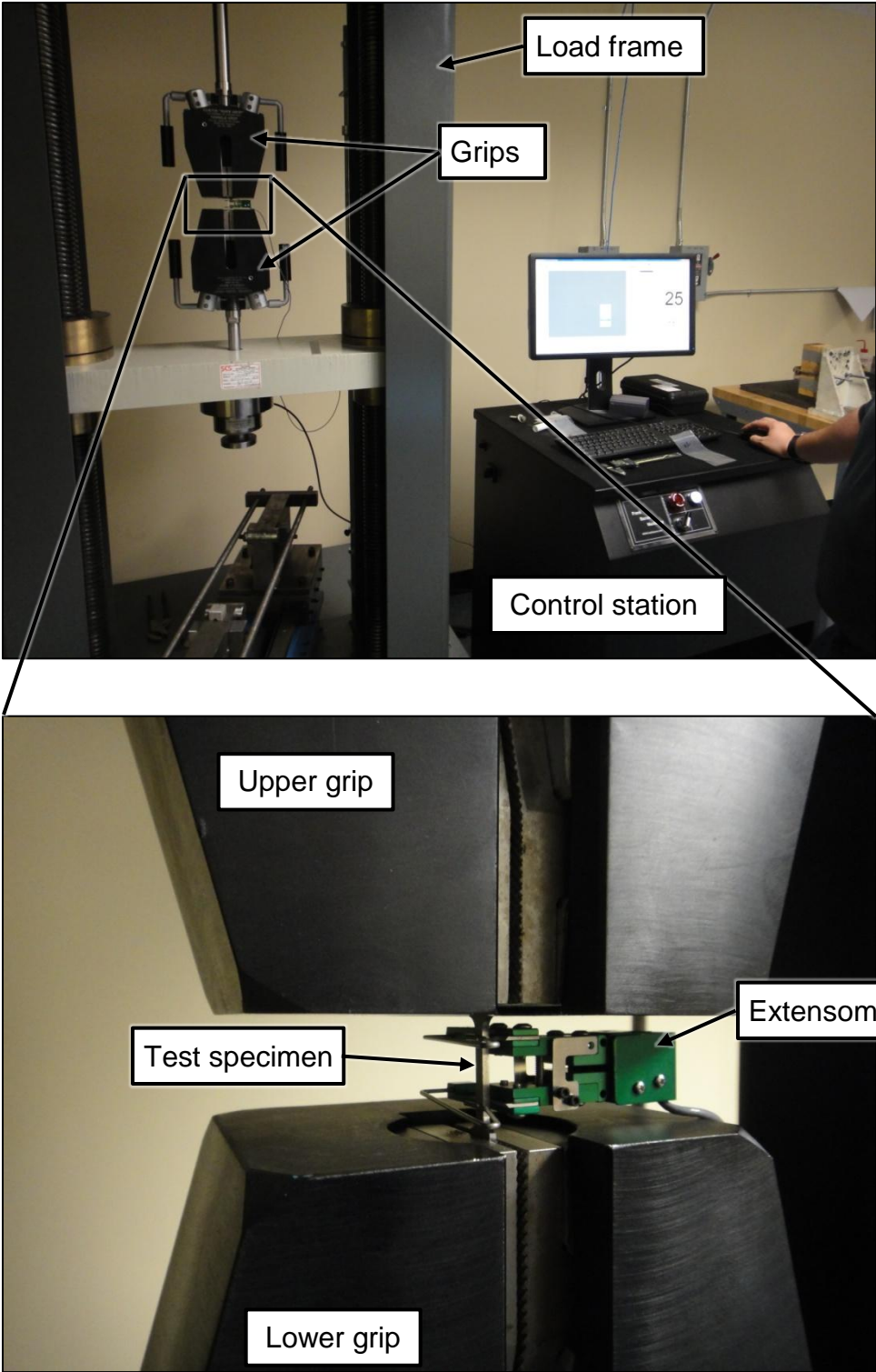


Figure 4. Overall view of the test frame (upper image) and the grip area (lower image) with a tensile specimen from the attachment ring loaded and ready to test.

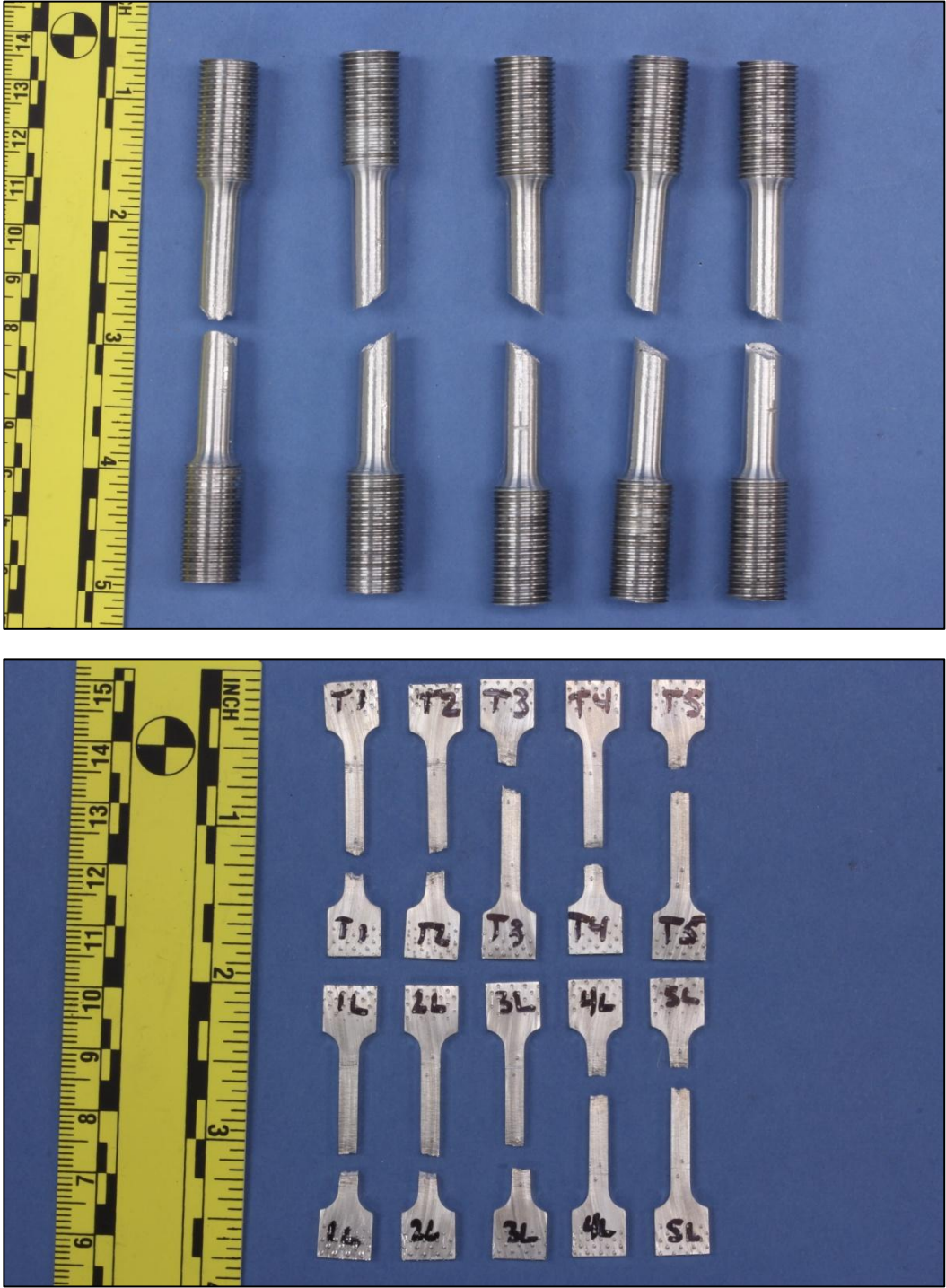


Figure 5. Overall view of the 5 standard round specimens (upper image) and the 10 custom flat specimens (lower image) from the test block after testing.

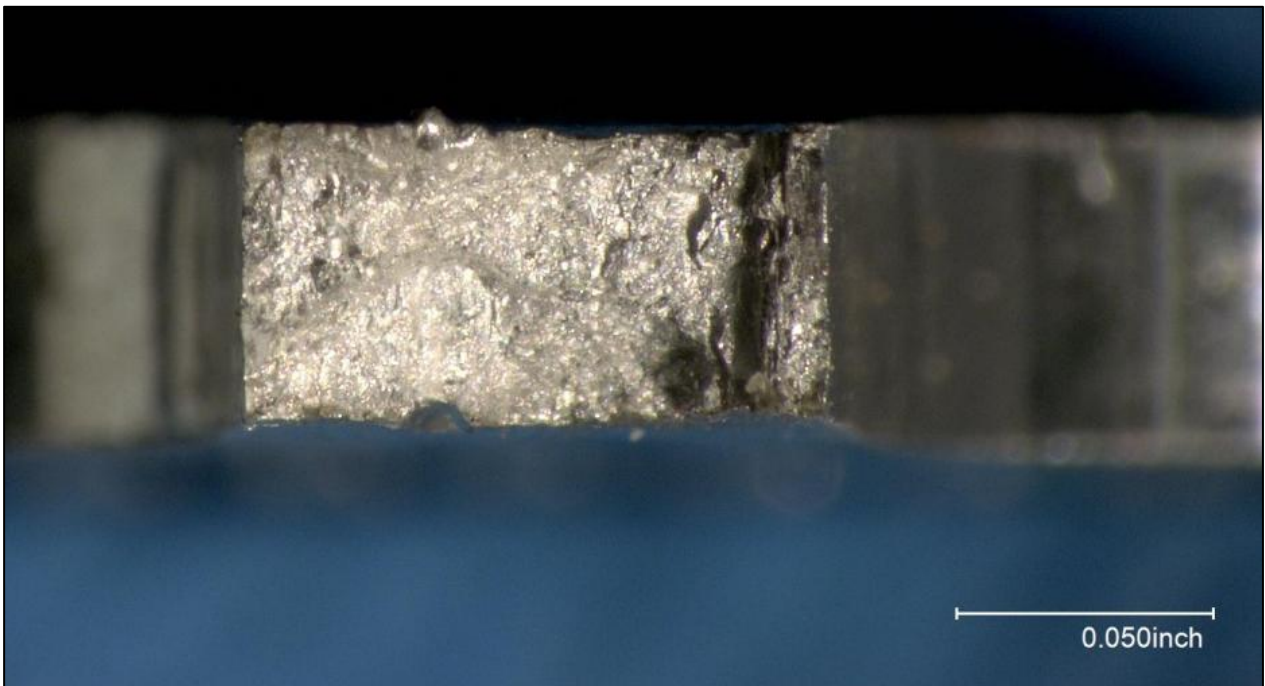
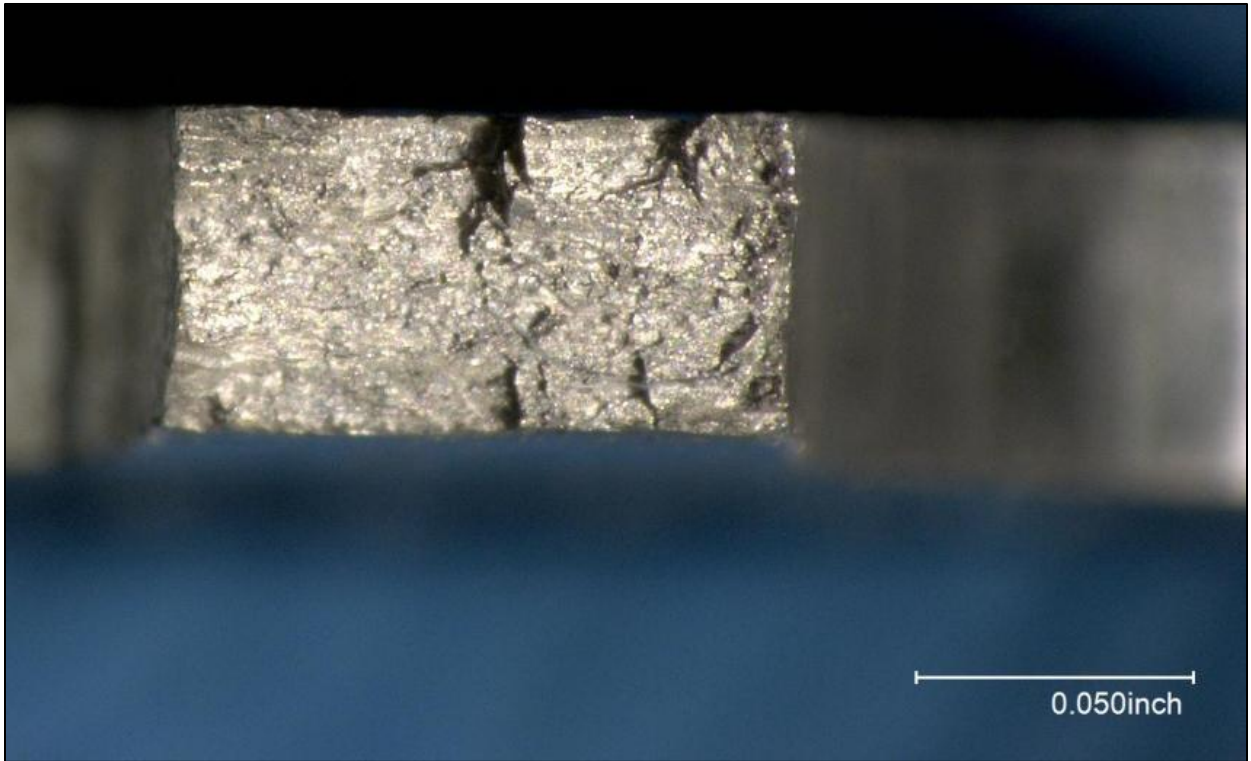


Figure 6. Optical views of fracture features on tensile specimens F1L (upper image) and F1T (lower image) from the test block.

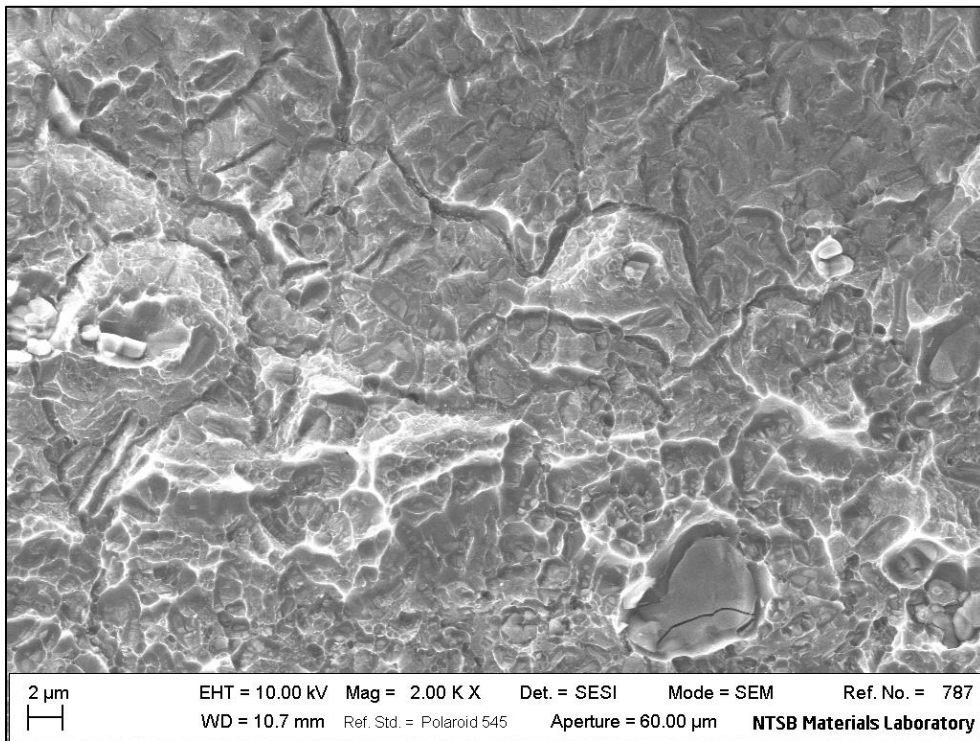
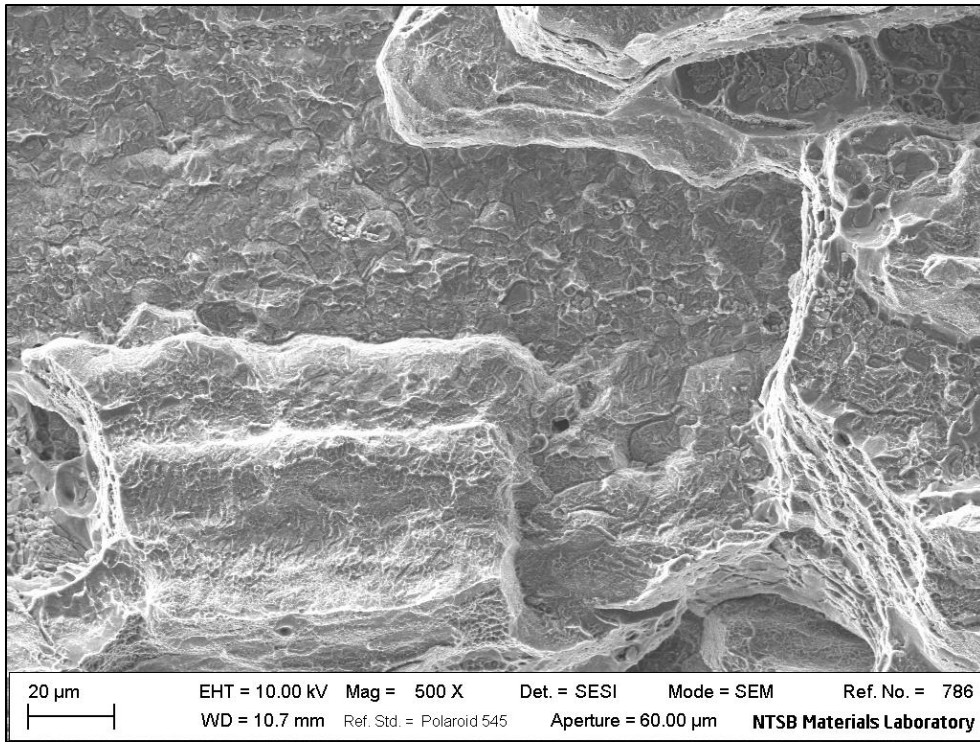


Figure 7. SEM images of typical features observed on the fracture surface of tensile specimen F1L.

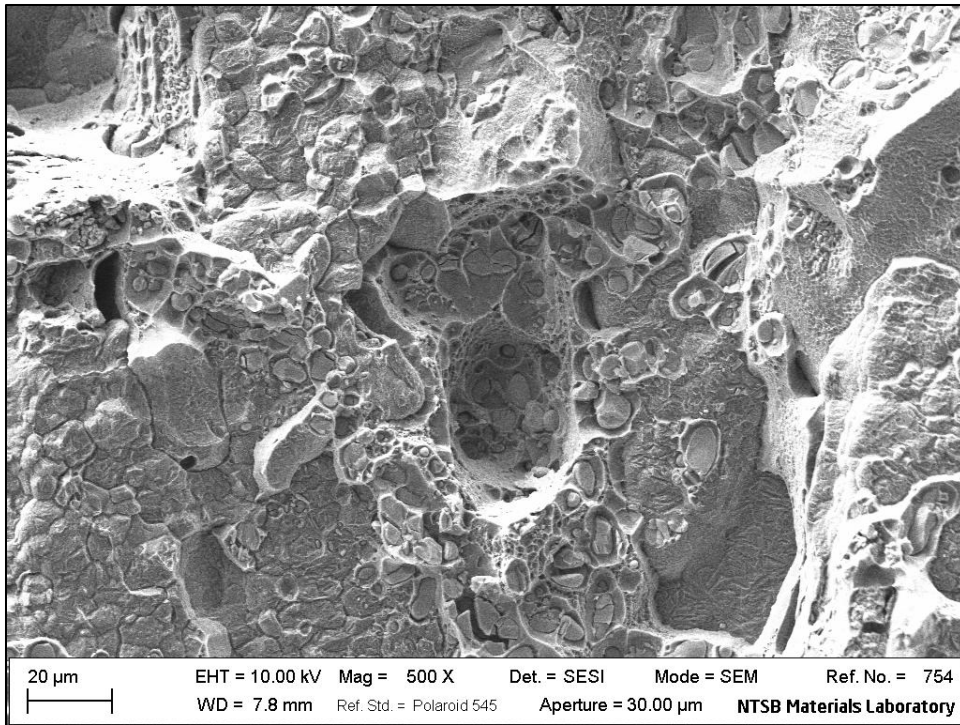


Figure 8. SEM image of typical features observed on the fracture surface of tensile specimen F1T.

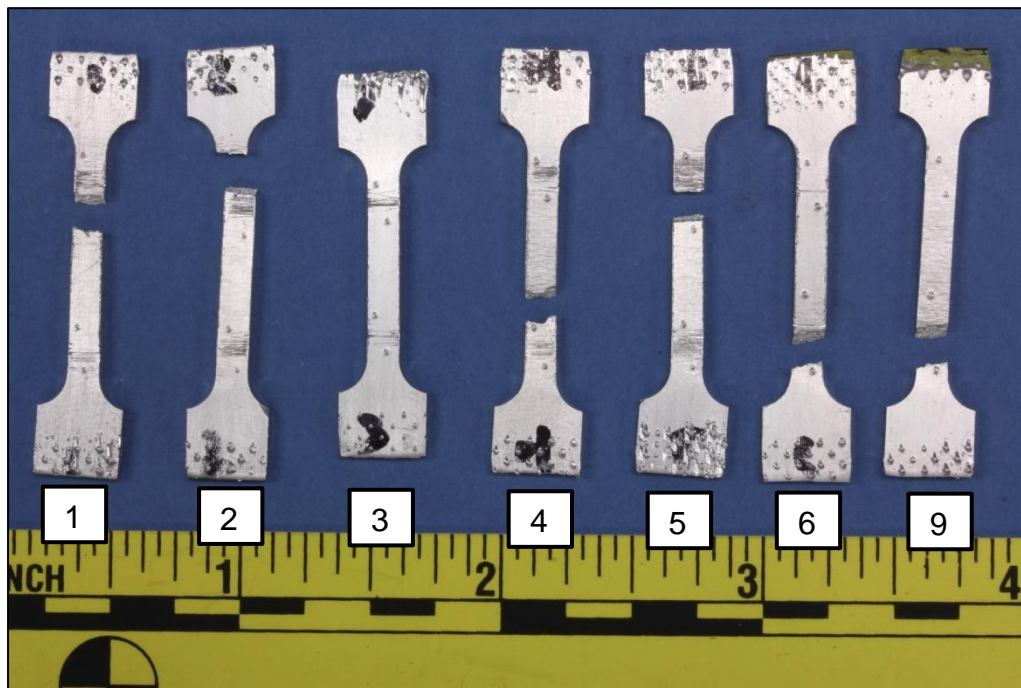


Figure 9. Overall view of the tensile specimens from the fenestron attachment ring after testing was completed.

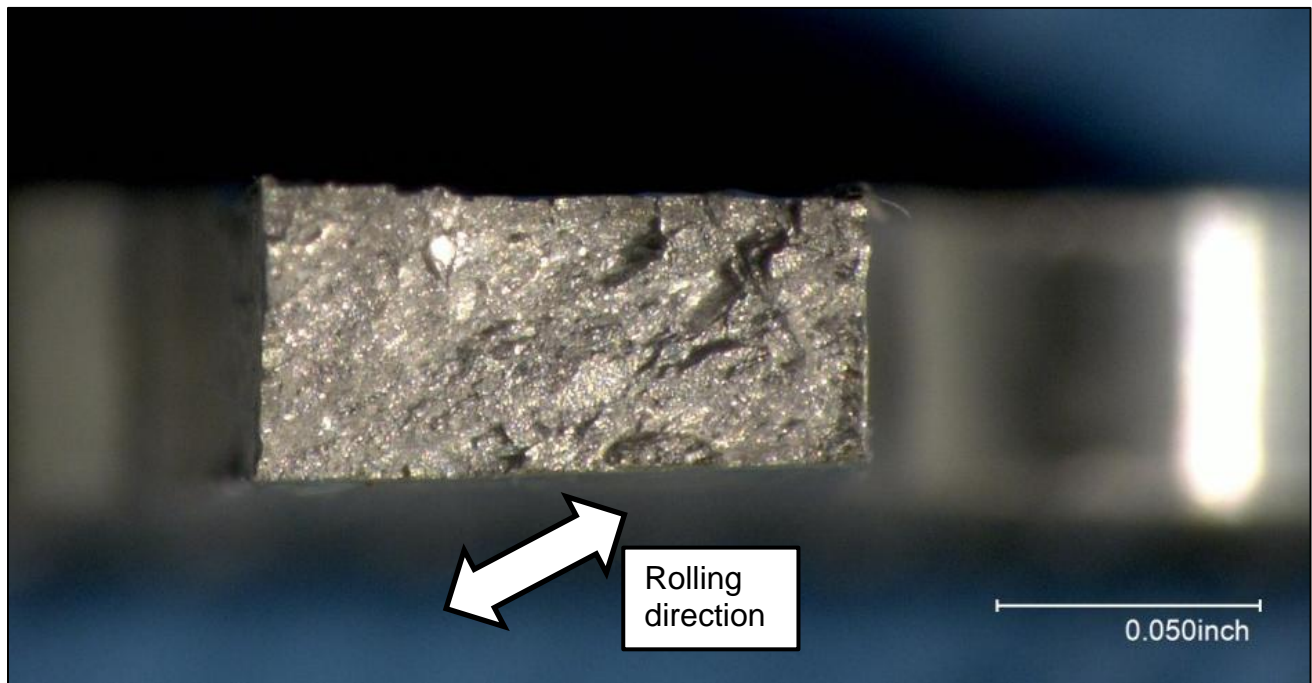
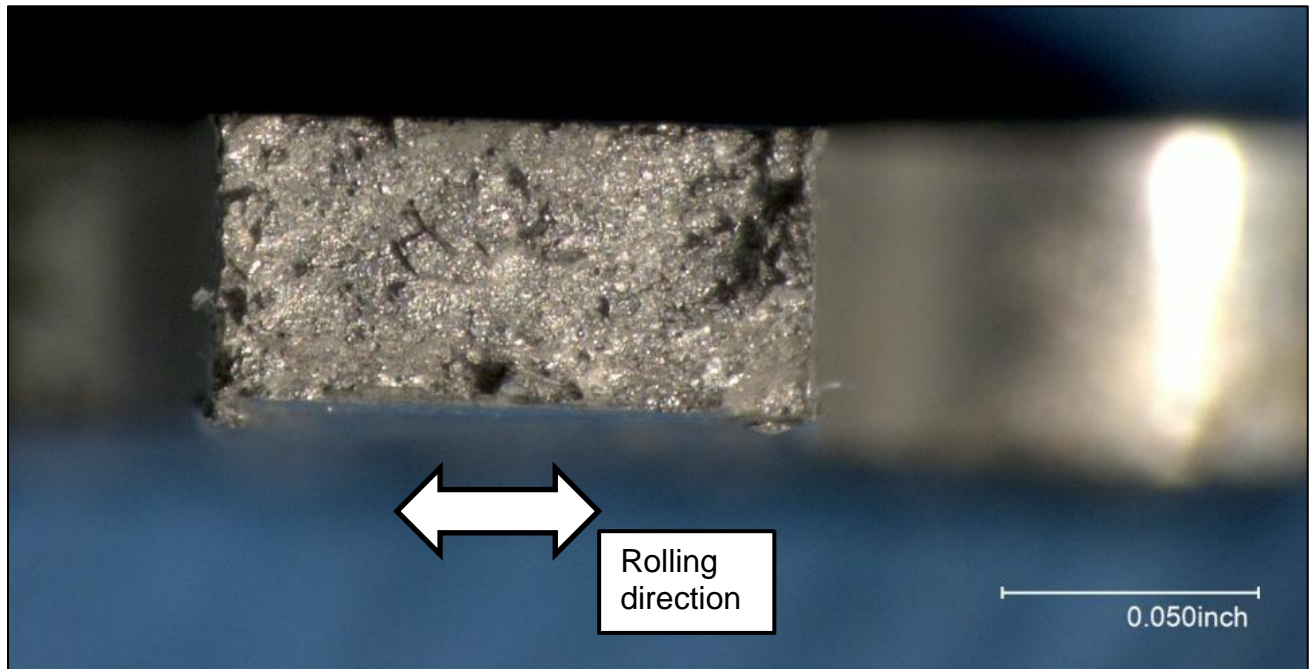


Figure 10. Optical views of fracture features on tensile specimens 1 (upper image) and 4 (lower image) from the fenestron attachment ring.

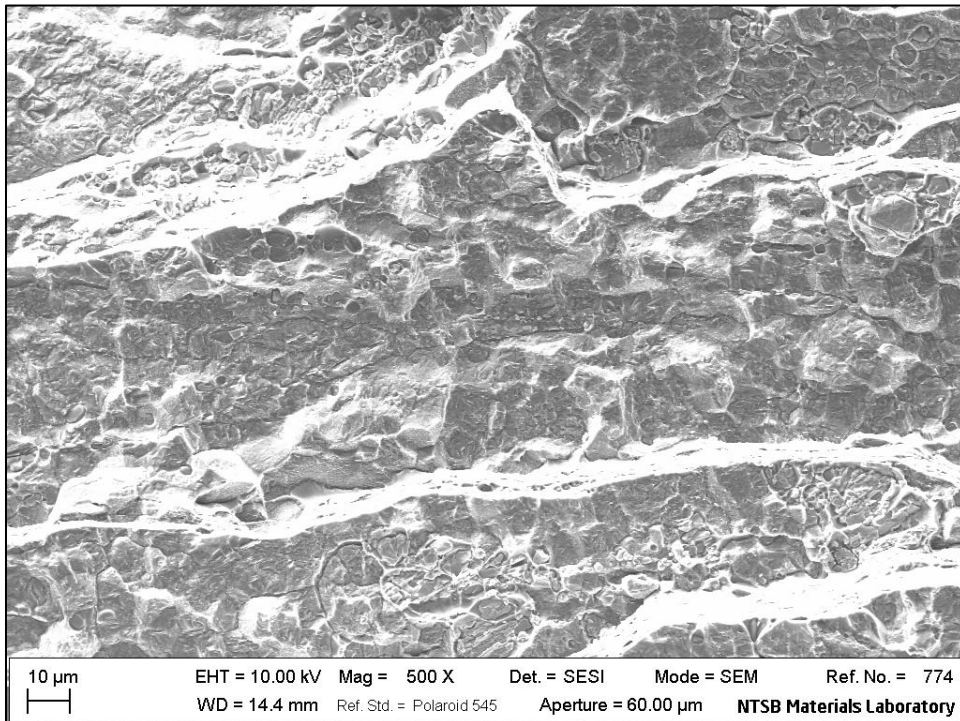
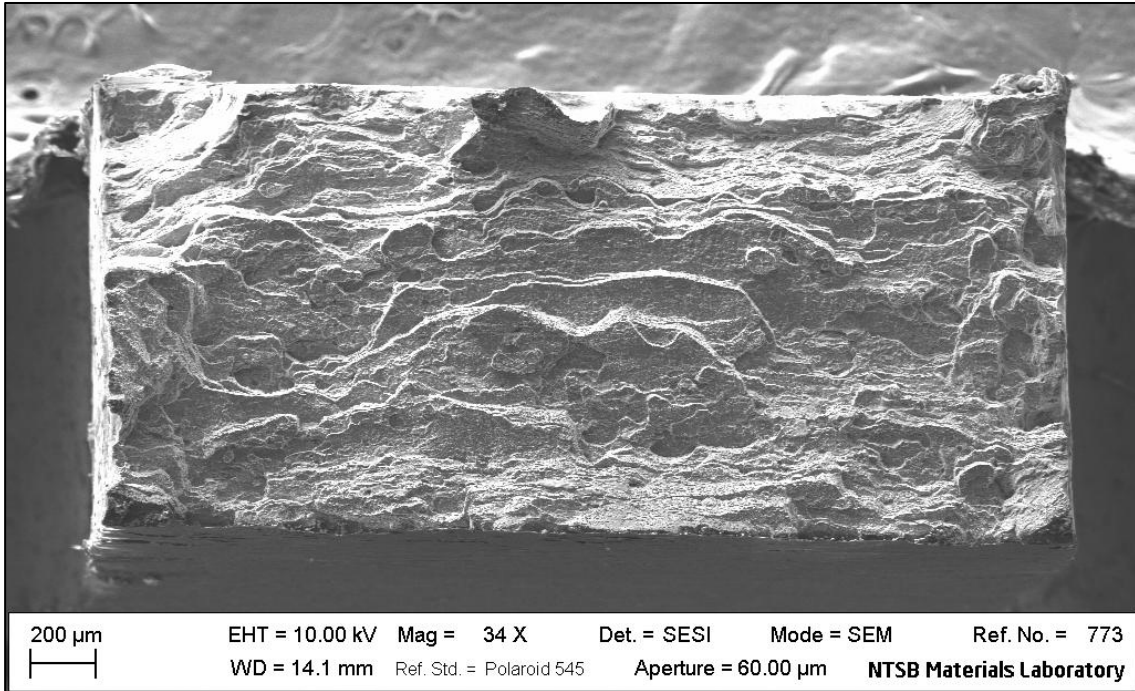


Figure 11. SEM images of Test Specimen 1 from the fenestron attachment ring showing typical fracture features.

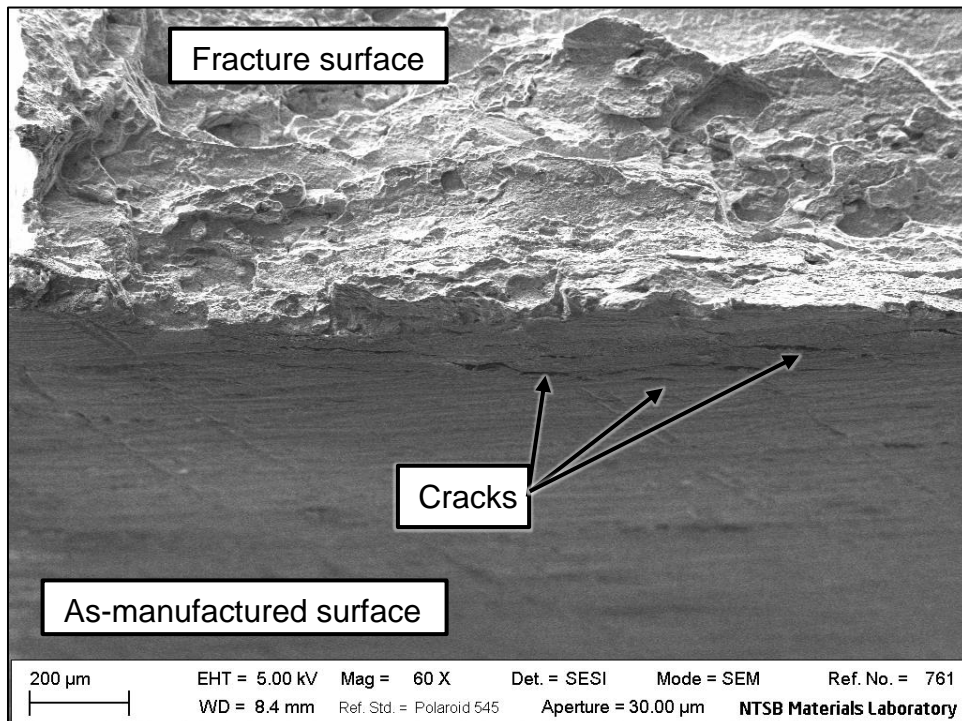
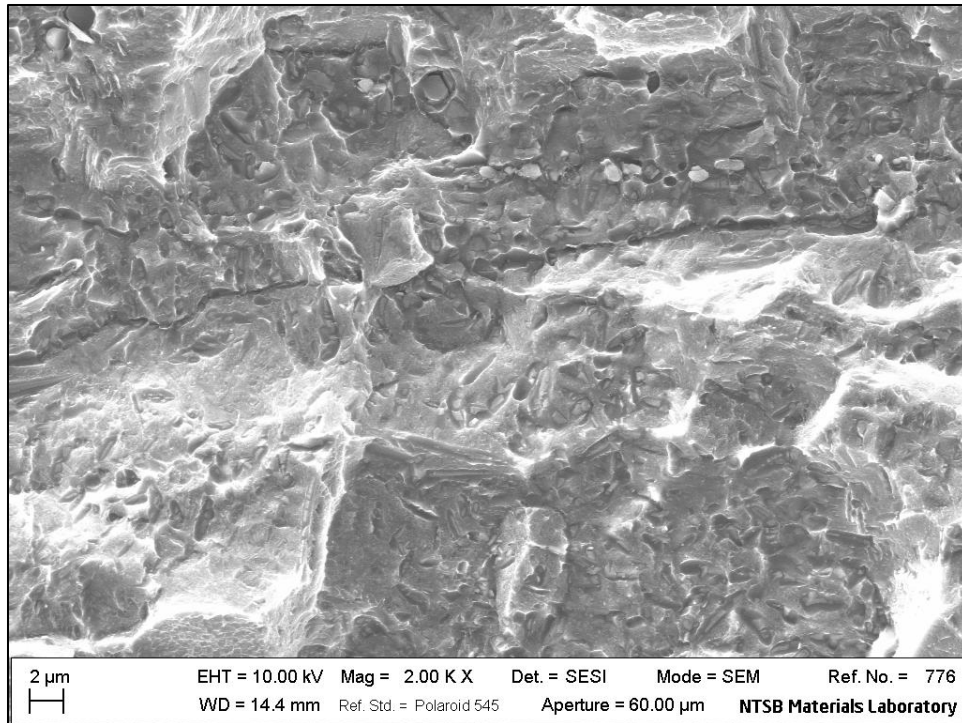


Figure 12. SEM images of Test Specimen 1 from the fenestron attachment ring showing typical fracture features (upper image) and an oblique view showing secondary cracks on the as-manufactured surface adjacent to the fracture surface.

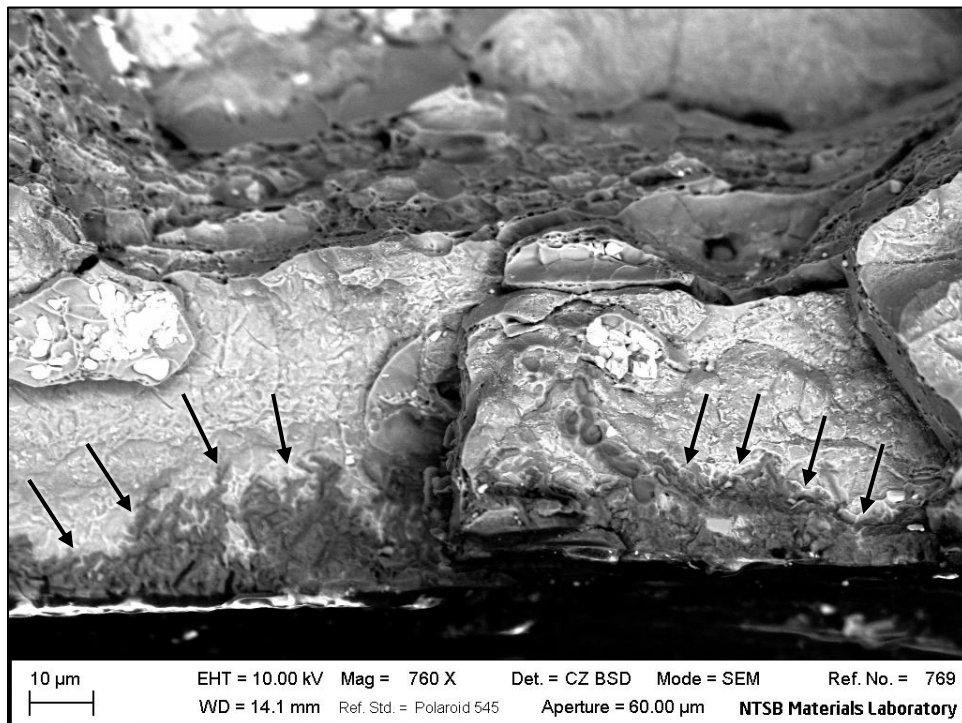
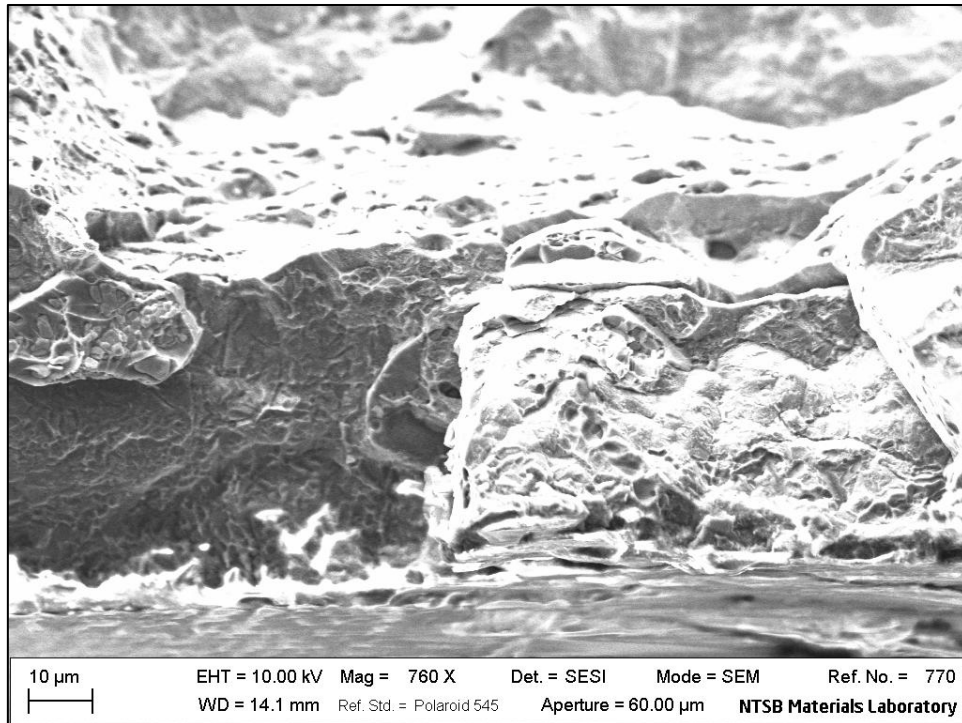


Figure 13. SEM images using secondary electrons (upper image) and backscattered electrons (lower image) to view the same area of the fracture surface on Test Specimen 1 adjacent to the as-manufactured surface. Darker areas indicated with arrows on the lower image are consistent with oxidized grain boundary etch pits.

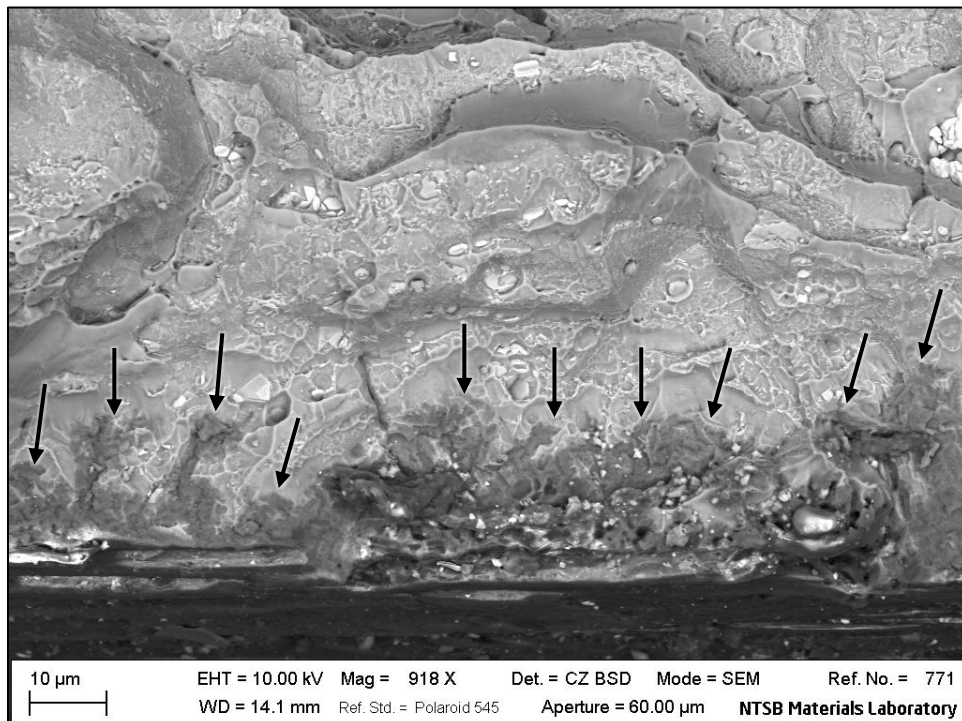
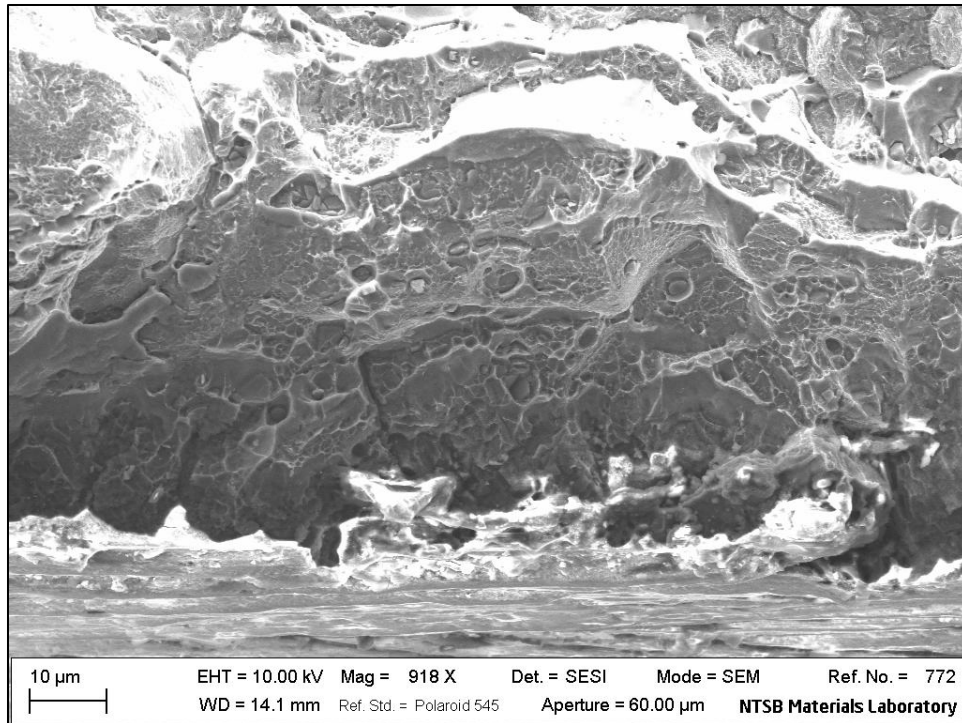


Figure 14. SEM images using secondary electrons (upper image) and backscattered electrons (lower image) to view the same area of the fracture surface on Test Specimen 1 adjacent to the as-manufactured surface. Darker areas indicated with arrows on the lower image are consistent with oxidized grain boundary etch pits.

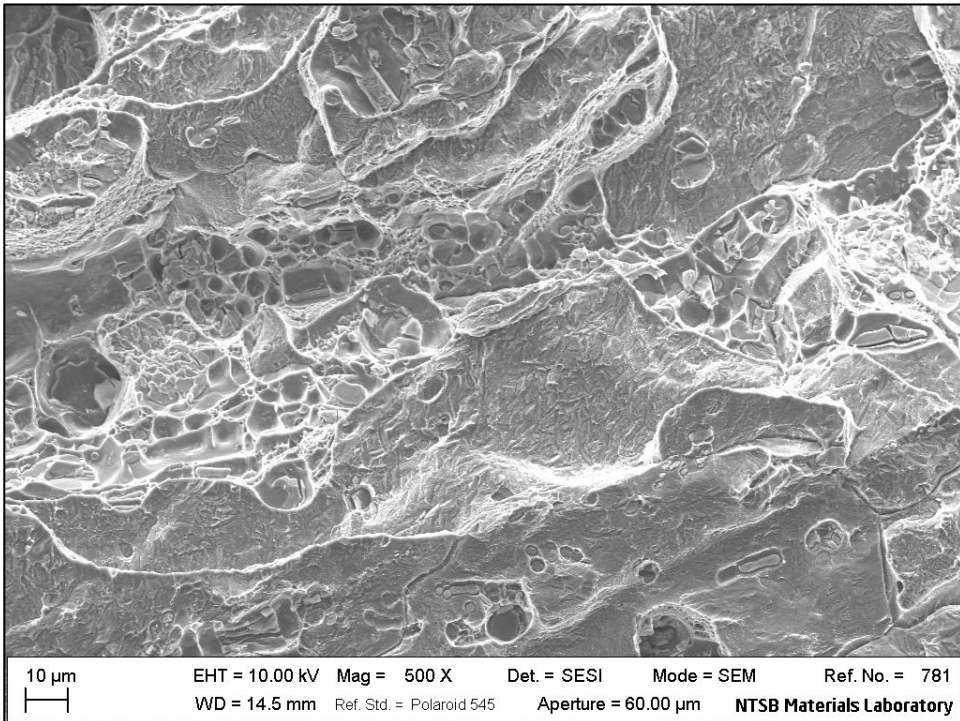
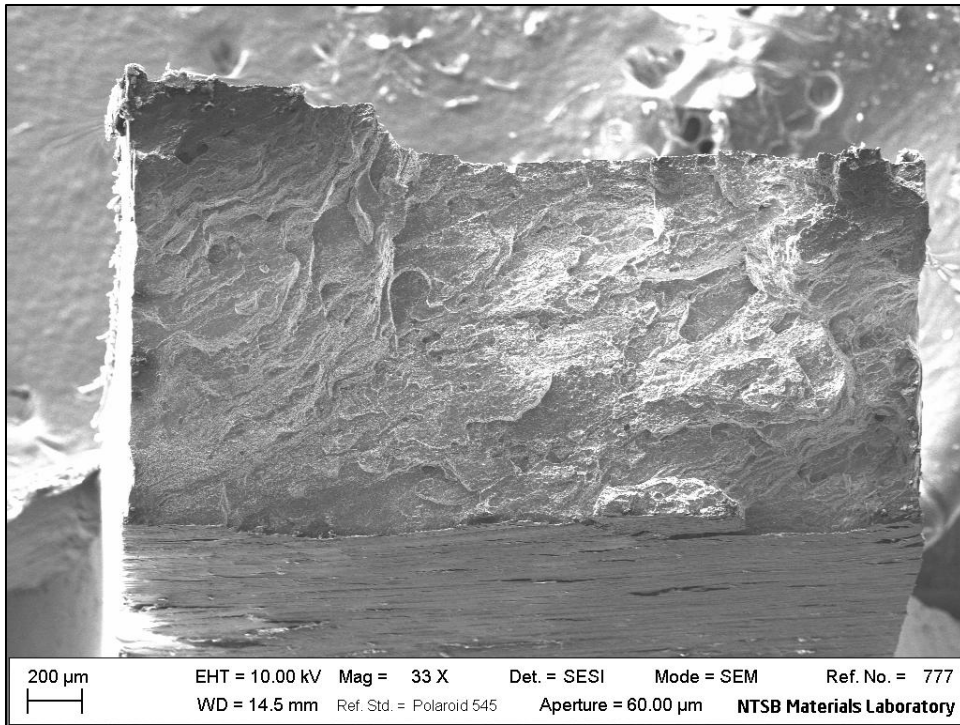


Figure 15. SEM images of Test Specimen 4 from the fenestron attachment ring showing typical fracture features.

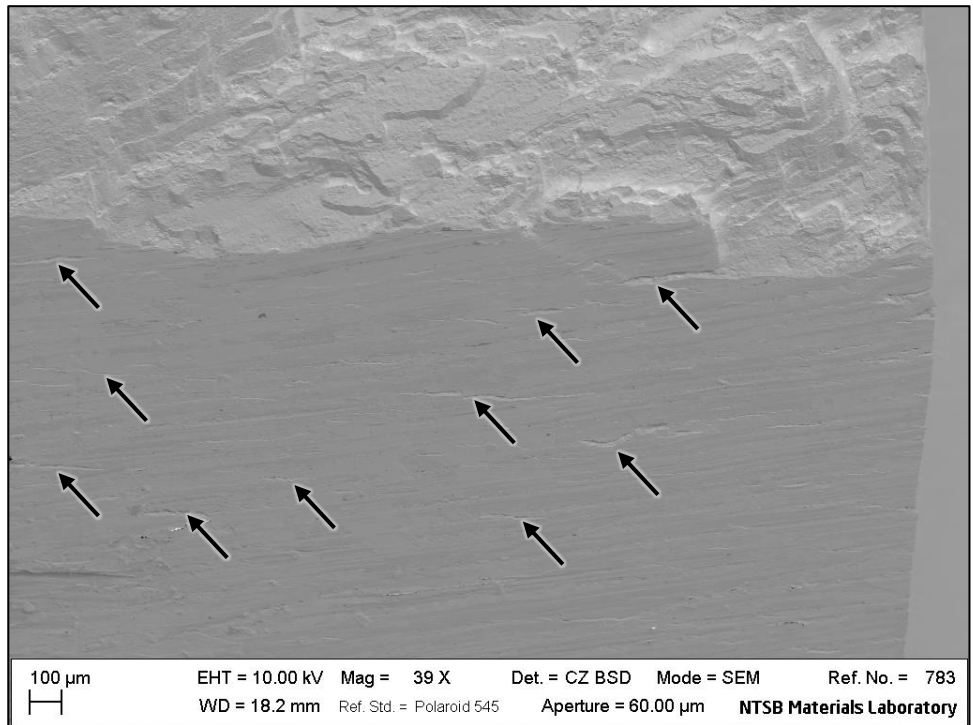
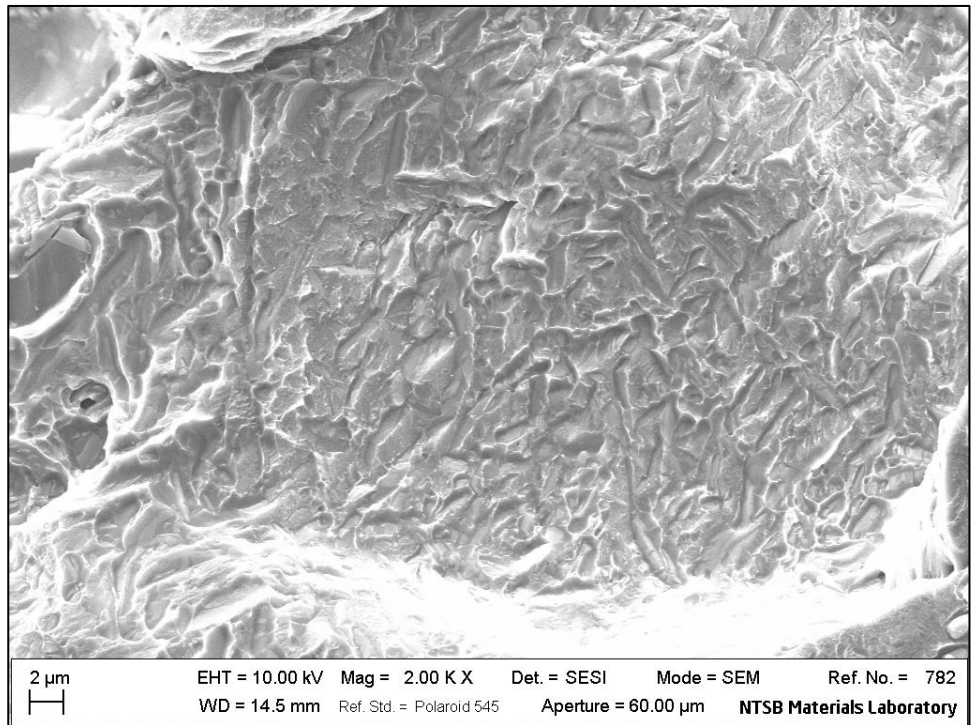


Figure 16. SEM images of Test Specimen 4 from the fenestron attachment ring showing typical fracture features (upper image) and an oblique view with arrows indicating some of the secondary cracks observed on the as-manufactured surface adjacent to the fracture surface.

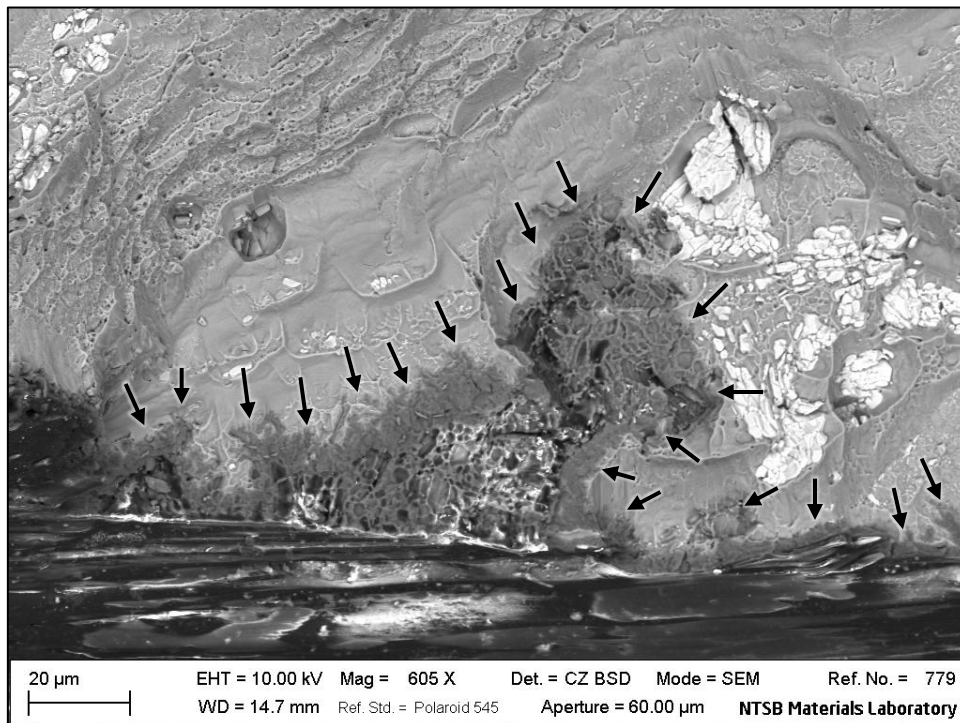
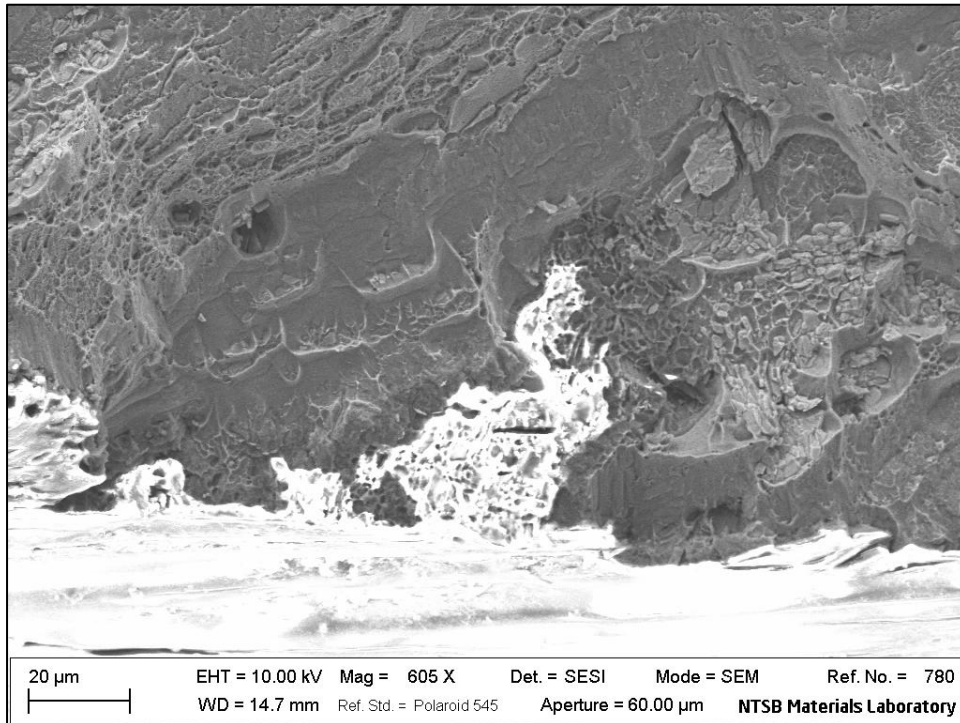


Figure 17. SEM images using secondary electrons (upper image) and backscattered electrons (lower image) to view the same area of the fracture surface on Test Specimen 4 adjacent to the as-manufactured surface. Darker areas indicated with arrows on the lower image are consistent with oxidized grain boundary etch pits.

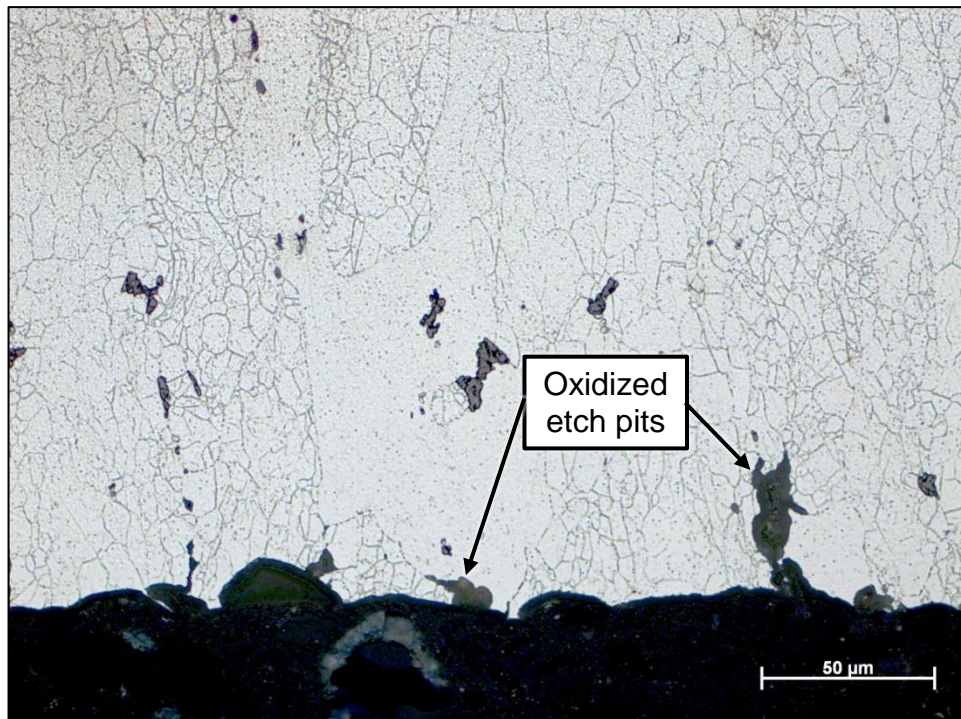
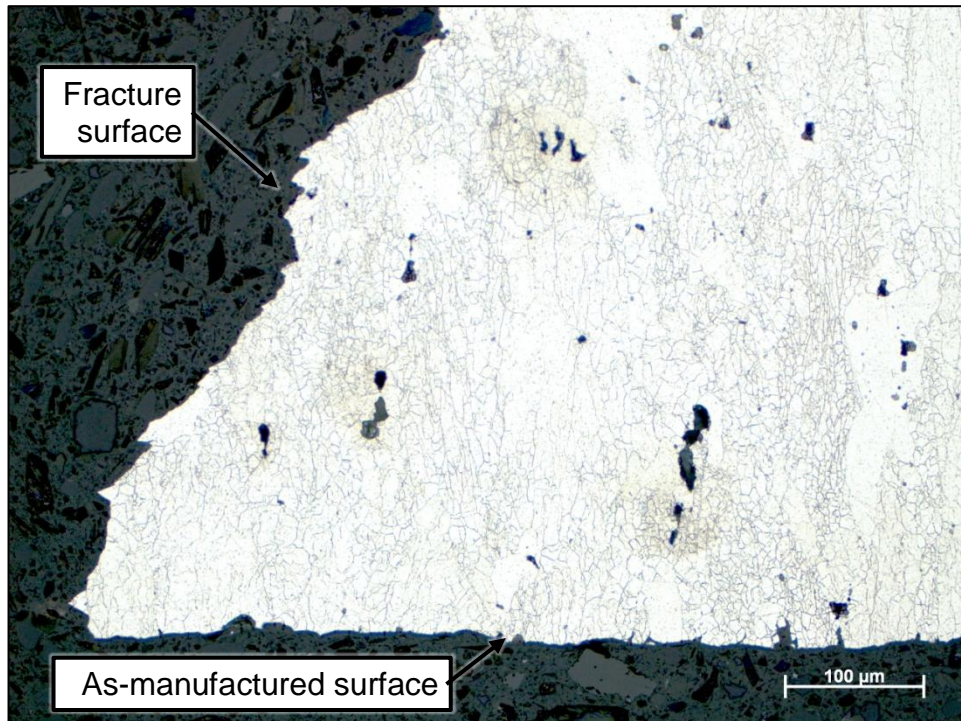


Figure 18. Views of the polished and etched (Keller's reagent) cross-section of test sample 1 showing the microstructure at the as-manufactured surface. The upper image shows the microstructure near the fracture surface, and the lower image shows one of the deepest oxidized grain boundary etch pits.

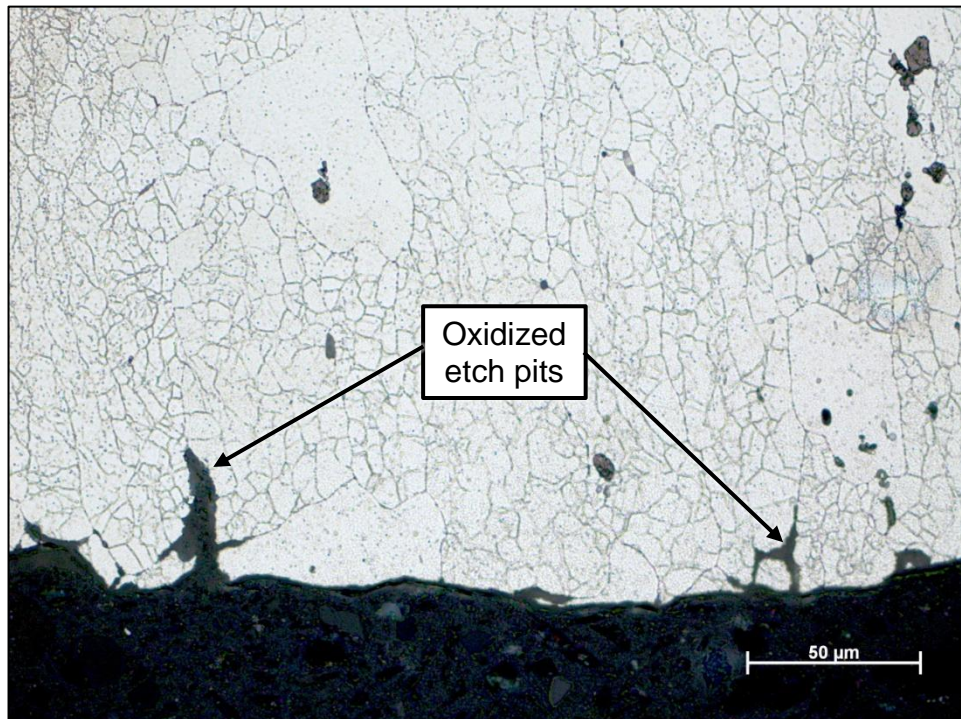
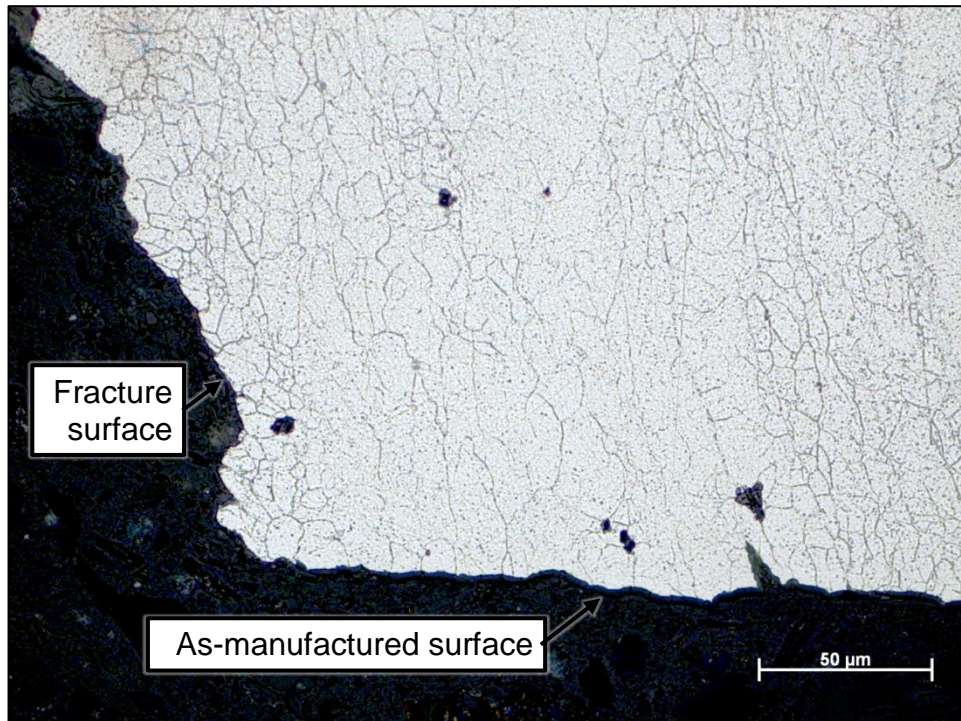


Figure 19. Views of the polished and etched (Keller's reagent) cross-section of test sample 4 showing the microstructure at the as-manufactured surface. The upper image shows the microstructure near the fracture surface, and the lower image shows one of the deepest oxidized grain boundary etch pits.